IEEE Access
Multidisciplinary ⋮ Rapid Review ⋮ Open Access Journal

Received 21 July 2023, accepted 14 August 2023, date of publication 17 August 2023, date of current version 23 August 2023.

Digital Object Identifier 10.1109/ACCESS.2023.3306337

APPLIED RESEARCH

1-Bit Reconfigurable Beam Steering Planar Array Antenna Based on Reflectarray Feeding

POORIA KABIRI, MOHAMMAD KHALAJ-AMIRHOSSEINI, AND ALI PESARAKLOO
Department of Electrical Engineering, Iran University of Science and Technology, Tehran 13114-16846, Iran
Corresponding author: Ali Pesarakloo (ali_pesarakloo@elec.iust.ac.ir)

ABSTRACT In this paper, we present a method for reducing the quantization lobe in a 1-bit beam steering planar array antenna. The method is inspired by reflectarray feeding in such a way that as we move away from the center of the array, the phase becomes more negative. This type of element phasing disturbs the periodicity of the quantization phase error and therefore suppresses the quantization lobe. Each 1-bit antenna element has two phase states (0 and 180°) that are provided through two symmetrical feeding points and are controlled with two PIN diodes. The planar array is fed by a series microstrip line network. One prototype of the proposed planar array with 8×8 elements was fabricated and tested at 3.4 GHz, which showed a measured scan range between $-45°$ and $+45°$ with a maximum quantization lobe level of -9 dB and a gain variation of 1.5 dB. The proposed 1-bit beam scanning antenna has a much simpler feeding network than other planar array antennas. The overall thickness of the proposed array antenna is only $0.045\lambda_o$, which has a much lower profile than 1-bit reconfigurable reflectarray and transmitarray antennas with the same specifications. This proposed antenna is a usable and suitable candidate for wireless communication applications.

INDEX TERMS 1-Bit quantization lobe, reconfigurable antenna, planar array, microstrip antenna, beam steering.

I. INTRODUCTION

Beam scanning array antennas are an essential part of wireless communication, 5G networks, imaging systems, etc. [1]. Conventional phased arrays have a high cost, complexity in the feeding network, high weight, and large size due to the number of phase shifters required for every antenna element [2]. Electronically reconfigurable array antennas that have recently been noticed can be a suitable alternative to phased array antennas due to their lower complexity. In these antennas, the phase delays applied to each element are quantized into a number of discrete phases, and these phases are electronically controlled using switches such as liquid crystal [3], varactor [4], and PIN [5] diodes. In this case, the desired phase is replaced with its nearest quantized phase available. Digitally reconfigurable arrays are divided into two types: 3D structures and planar structures.

Reflectarrays [6], [7], [8] and transmitarrays [9], [10], [11], [12] are 3D structures that consist of a horn antenna as a feed and reflective or transmissive array elements. In [6], a 14 × 14 1-bit reflectarray was designed based on PIN diode with a scanning range of ±60° for X band. In [8], Luyen et al. presented a new method for achieving 2-bit phase quantization for beam-steerable reflectarrays by exploiting four distinct reflection modes of a unit cell. Simulations predict good performance in the scan range of ±45° in the H-plane, with a maximum gain variation of 3.0 dB over the frequency range of 9-11 GHz. In [11], a 1-bit 20 × 20 circularly-polarized reconfigurable TA in the Ka-band was designed with a scanning range of ±60°. In [12], a 2-bit 14 × 14 TA was presented with a 19.8 dB max gain and ±60° beam scanning. These structures are bulky, with a thickness of several wavelengths, and therefore cannot be used in space-limited applications such as satellite communication. In addition, the feeding structure in reflectarray and transmitarray antennas has illuminating and spillover losses, which lead to the reduction of aperture efficiency in these antennas. In addition to these cases, losses due to the blockage of the feed horn are also present in reflectarray antennas.

The associate editor coordinating the review of this manuscript and approving it for publication was Debabrata K. Karmokar.

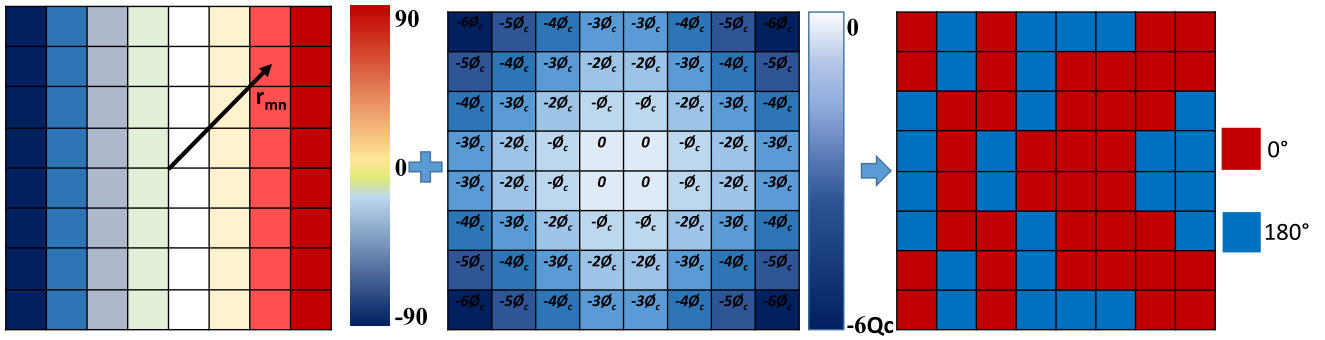

FIGURE 1. (a) Excitation phase obtained from (1) for the direction of (θ_0, 0), (b) phase delay obtained from (3) and (c) total phase after quantization.

The second type of digitally reconfigurable arrays is planar arrays that are fed by a microstrip line network, and unlike 3D structures, they are low profile and simple structures [13], [14], [15], [16]. A planar 4-bit reconfigurable antenna array based on the design philosophy of information metasurfaces was proposed in [16] with a scanning range of $\pm 45°$ range and a 13.4dB gain in broadside. In [15], a 2-bit 8-element planar traveling wave array antenna was presented that steers one beam. The measured results show that the proposed array can scan from $-49°$ to $+49°$ and maintains an acceptable 3 dB AR bandwidth in the desired band around 3.65 GHz.

To decrease the complexity, weight, and size of the array, it is preferable to reduce the number of bits.

In digitally controlled array antennas that use two-bit phase shifting and above, a single beam is always created in the radiation pattern. But when the phase shifting is of 1-bit type, single-beam can only be achieved if there is an intrinsic pseudo-random distribution of the phase quantization error. The phase quantization error is defined as the difference in the ideal and discretized phase of the elements. In reflectarray and transmitarray antennas this pseudo-random distribution is created automatically due to the different spatial paths from the feeding source to each element. But in conventional planar arrays with 1-bit phase shifting, due to the lack of this random phasing, we always see two beams with the same amplitude [17].

In [18], a wideband 1-bit 4×4 digital-controllable patch array antenna with dynamic beam manipulation capability was developed. In [19], a low-profile and high-gain pattern reconfigurable 1-bit planar array antenna based on digital coding characterization was presented. In both works, two beams are scanned simultaneously; therefore, they are not suitable for scanning applications because of the quantization lobe error.

To the best of our knowledge, few works have been done on 1-bit single-beam planar array antennas until now. In [20], a new architecture for low-cost single-beam planar array antennas suitable for linear-polarized satellite communication systems was presented. The approach is based on the use of 1-bit phase controls that can be implemented using discrete components and on an aperiodic sunflower-like arrangement of the elements. A 48-element prototype has been designed, built, and measured at Ku-band with a scanning range of $\pm 30°$. However, the presented array and proposed feeding network are very complex to implement.

In this paper, a 1-bit planar array antenna with single-beam scanning in a wide angular range is proposed. The idea behind this work is to assign to each element a predetermined phase inspired by reflectarray feeding. The distribution of this predetermined phase is such that the phase delay further increases as the distance from the center of the structure increases. The proposed antenna consists of two layers, with the antenna elements placed in the upper layer and the feeding network placed in the lower layer. The feeding network is of series-fed type, and the predetermined phases are implemented using delay lines included in the feeding network. This feeding network is much simpler than the feeding networks used in other planar array antennas. The overall thickness of the proposed planar array antenna is $0.045\lambda_o$, which indicates that the antenna is very low profile.

II. THEORETICAL BACKGROUND

Let us consider a conventional 1-bit planar array antenna consisting $M \times N$ elements that are excited with a microstrip feeding network. To achieve a main beam in the direction of (θ_0, φ_0), the required phase of the mn^{th} element is given by:

$$\Phi_{mn} = -k\sin\theta_0(x_m\cos\varphi_0 + y_n\sin\varphi_0) \tag{1}$$

where k is the free space wavenumber and (x_m, y_n) is the coordinate of each element. A schematic of the excitation phase Φ_{mn} for the main beam direction of (θ_0, 0) is shown in Figure 1(a). In 1-bit phase shifting, the required phase of each element is quantized to 0° and 180° by the following relation:

$$\Phi^q_{mn} = \begin{cases} 0°(0), & -90° \le \Phi_{mn} \le 90° \\ 180°(1), & \text{otherwise} \end{cases} \tag{2}$$

without losing the generality of the problem, it is assumed that the direction of the main beam is (30°, 0°) and M=N=8. In this case, the phase distribution of the conventional

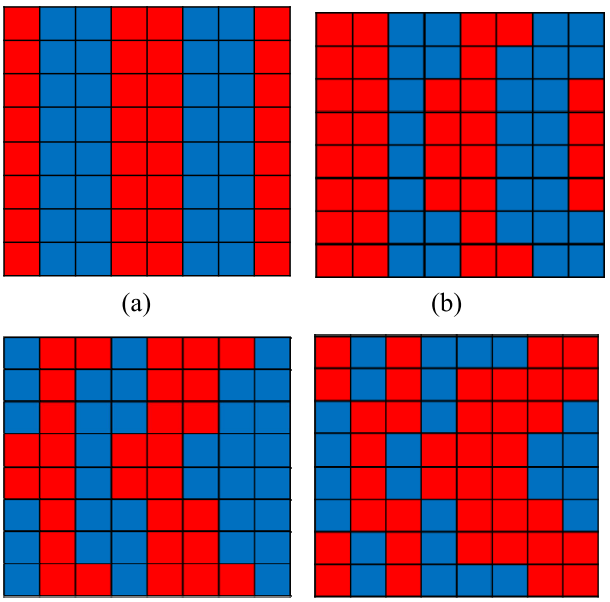

FIGURE 2. Distribution of quantization phase for the scan angle of (30°,0°) obtained from (3) with a) Φc =0°, b) Φc =15°, c) Φc =30°, d) Φc =60°.

1-bit planar array, which is obtained using Equations 1 and 2, is shown in Figure 2(a). The radiation pattern of this phase distribution is obtained from the array factor theory and is shown in Figure 3(a). As can be seen, a secondary beam of the same magnitude as the main beam appears in the opposite direction called the quantization lobe. This is due to the periodicity of the phase distribution along x-direction.

Now, a compensating phase inspired by reflectarray antennas is added to the elements in such a way that the phase delay further increases as the distance from the center of the structure increases, and the elements that are at the same radial distance from the center of the array get the same phase, as shown in Figure 1(b). In this case, the total phase of each element is as follows:

$$\Phi_{mn}^{Total} = -k\sin\theta(\mathrm{x_m}\cos\varphi + \mathrm{y_n}\sin\varphi) - \Phi_{mn}^{comp}$$
$$\Phi_{mn}^{comp} = -n \times \Phi_c, \quad n = \left\lfloor \frac{r_{mn}}{P} \right\rfloor \tag{3}$$

where $\lfloor\cdot\rfloor$ is the floor (round down) operator, Φ_c is a constant phase, $r_{mn} = \sqrt{x_m^2 + y_n^2}$ and P is inter-element spacing. A schematic of phase delay Φ_{mn}^{comp} is shown in Figure 1(b). When this distribution phase is quantized, the periodicity of the distribution of quantized phases is broken and therefore the quantization lobe is reduced. To verify the proposed method, we change Φ_c from 0° and investigate its effect on the quantized phase distribution and radiation pattern. In this case, the array factor of the planar array is given by

$$AF(\theta,\varphi) = \frac{1}{MN}\sum_{m=1}^{M}\sum_{n=1}^{N}\exp\left[\begin{matrix} jk_0(x_m\sin\theta\cos\varphi + y_n\sin\theta\cos\varphi) \\ +j(\Phi_{mn}^{q} + \Phi_{mn}^{comp}) \end{matrix}\right] \tag{4}$$

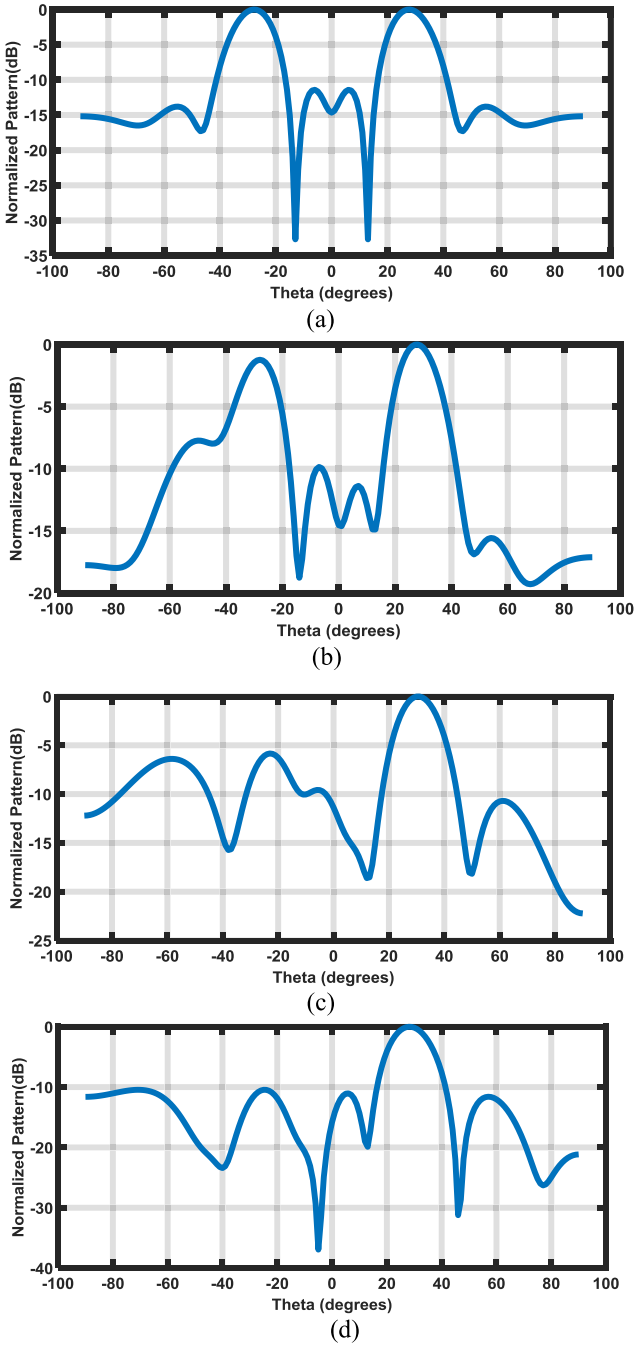

FIGURE 3. The radiation pattern of 8 × 8 planar array for the scan angle of θ =30°, ϕ =0° obtained from (3), (4) with (a) Φc =0°, (b) Φc =15°, (c) Φc =30°, and (d) Φc =60°.

First, Φ_c is selected 15° and the quantized phase distribution and radiation pattern are plotted as shown in Figure 2(b) and 3(b), respectively. As can be seen, the periodicity of the phase distribution along x-direction is slightly broken that causes the quantization lobe level (QLL) to be reduced by 1.5dB. When Φ_c increases to 30°, the quantized phase distribution changes further, resulting in a QLL of −6.5dB as depicted in Figures 2(c) and 3(c), respectively. By increasing Φ_c again to 60°, the quantization lobe decreases noticeably and reaches the value of QLL=-11.6 dB, as shown

in Figure 3(d). This results from the highly non-periodic phase distribution shown in Figure 2(d). When Φc is 60°, the full range of phase (0°-360°) is utilized by the elements in the 8 × 8 array antenna. Therefore, by increasing the phase more than 60°, there is no further improvement in quantization lobe reduction.

To illustrate the capability of the design for beam scanning, the performance of the design for other main beam directions and Φ_c =60° is evaluated. The normalized radiation pattern of the array for the main beam direction of 20° is presented in Figure 4, which shows a QLL of −11.8 dB. Thus, it is evident that the proposed technique has excellent quantization lobe reduction capabilities irrespective of the directions of the main beam.

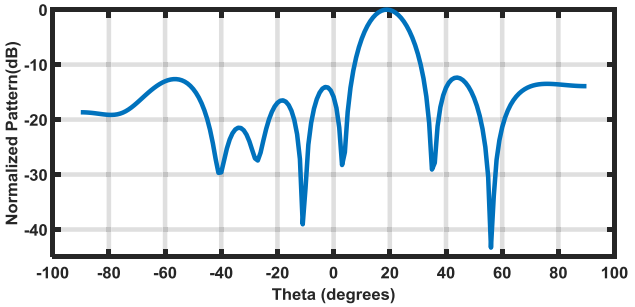

FIGURE 4. The radiation pattern of the proposed planar array for the scan angle of θ =20°, ϕ =0° with Φc =60°.

A critical issue in phased array antennas is scan blindness. If an infinite array structure is capable of supporting a guided wave (here, a patch array in which the guided wave mode is the surface wave mode that is supported by the dielectric substrate layer), then under certain Floquet excitations, the propagation constant of a surface wave mode coincides with that of a Floquet mode. In this case, these two modes couple strongly, leading to a resonance and subsequent scan blindness [21], [23]. The scan blindness phenomenon in the phased array antennas occurs under following conditions [21], [22], [23]:

- The array must have a Floquet excitation, that is, the elements should be excited with uniform amplitudes and linearly progressed phase.
- The element must reside in an infinite array environment. But the analysis of finite arrays shows that even small arrays (3 × 3 or 7 × 7) can have dips in the element pattern where the infinite array has a scan blindness, and that this effect becomes more pronounced as array size increases.

But in the proposed 1-bit digitally reconfigurable array, the required phase of each element to scan the beam to a specific angle is first summed with a compensating phase inspired by reflectarray antennas (Φ_{mn}^{comp}). This compensating phase is added in such a way that the phase delay increases further as the distance from the center of the structure increases, and the elements that are at the same radial distance from the center of the array get the same phase. Next, the sum of these two phases is quantized into 0° and 180°. Consequently, the quantized phase and therefore the excitation phase of the elements, which is the sum of the quantized phase and the compensating phase, are distributed as a non-linear phase progression across the aperture of the array, preventing Floquet excitation and avoiding the scan blindness phenomenon.

III. DESIGN AND SIMULATION OF 1-BIT PLANAR ARRAY

A. 1-BIT ELEMENT

The configuration of the proposed 1-bit linear polarization element is schematically illustrated in Figure 5. The element consists of two layers of F4B substrate (ε_r = 2.56, tan δ = 0.002) with the dimensions of Ws×Ls. The patch element with the dimensions of Wp×Lp is located on the top layer and the transmission line as well as two PIN diodes are located on the bottom layer. The ground plane is located between two layers. The height of the top and bottom layers are h_1 =3 mm and h_2 =1 mm, respectively. The dimensions of the antenna element structure are presented in Table 1. The thickness of the patch and ground layers is 0.035mm and the ground plane is defected at two points to excite the patch using two vias with the radius of R. The input impedance of this 1-bit element is 50Ω.

Two PIN diodes on the bottom layer provide a 1-bit phase state for each element of the array antenna. By changing the ON/OFF state of the diodes, a 180° phase difference is obtained between the current excitation on the antenna elements by two via feeds. In simulations, the PIN diode is modeled as a lumped element. ON state is modeled as a 5 Ω resistor and the OFF state is modeled as a 0.05 PF capacitor. Figure 6(a) shows the current distribution on the patch layer by via1, and Figure 6(b) is the current distribution by via2. The current directions of the "0" and "1" states are exactly opposite, which means that there is a 180° phase difference between the two vias.

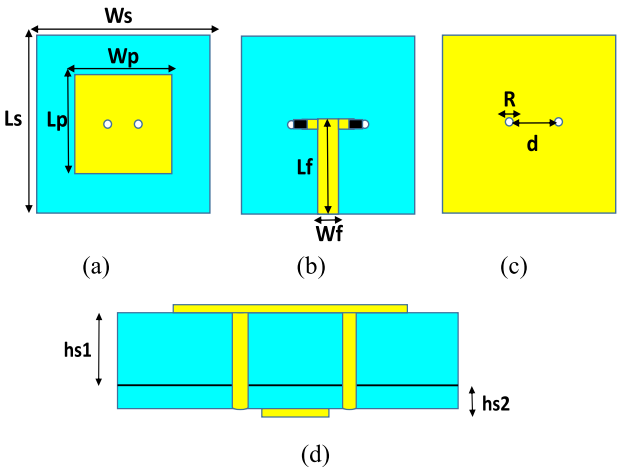

FIGURE 5. The geometry of the proposed 1-bit element, (a) top layer, (b) bottom layer, (c) ground plane, and (d) Cross-sectional topology.

The full-wave simulations and optimizations of antenna parameters are carried out by CST studio software. The return

TABLE 1. Geometrical parameters of single antenna structure (unit: mm).

W_S	L_S	W_p	L_p	W_f	L_f	R	d
40	40	24.9	24.9	2.84	20.5	0.5	9.6

loss of the 1-bit antenna element is shown in Figure 7(a). As can be seen, the operation frequency of the patch is 3.4GHz. The radiation properties of the element at 3.4 GHz are plotted in Figure 7(b) that shows the realized gain of 6.25 dB and the difference between co- and cross-polar radiations is at least 35 dB. Figure 7(c) shows the maximum realized gain in the range of 3.2GHz to 3.6GHz. As shown, in the range of 3.25 to 3.5 GHz, the gain is above 6 dB.

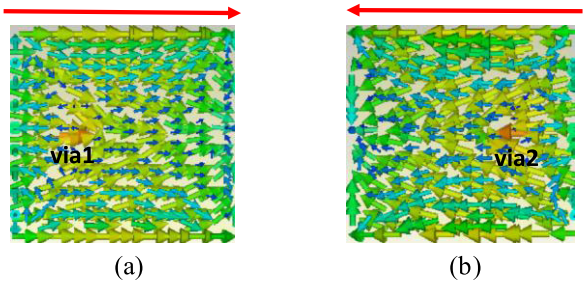

FIGURE 6. The surface current distribution of the proposed patch antenna element (a) Excited through feeding point V1(state 1), (b) Excited through feeding point V2(state 0).

Here, to realize the delay phases associated with each element, meander lines are used, as shown in Figure 8. By changing the length of the ΔL we can provide the specific phase delay. This length is calculated from (5). For example, for $\Phi_c = 60^\circ$ the length of the line is ΔL=8mm.

$$\Phi_{mn}^{comp} = \frac{\beta}{\Delta L_{mn}}, \quad \beta = \frac{2\pi}{\lambda_g} \tag{5}$$

B. FEEDING NETWORK

The feeding network used in this design must be capable of providing delay lines that correspond to the phase delay of each element. With a corporate feeding network, each element is fed separately, but the side elements of the array have large phase delays and therefore require large delay lines. This can cause space limitations during implementation. However, with a series feeding network, this issue is resolved because the large phase delays of the side elements are divided along the feeding network. This feeding network for the 1×4 array is shown in Figure 9(a). As we move from port 1 to port 5, the phase of each antenna element becomes more negative, such that the phase delay of port 2 is 0, port 3 is $-\Phi_c$, port 4 is $-2\Phi_c$, and port 5 is $-3\Phi_c$. Impedance matching at the branching point of the antenna elements is achieved using quarter wavelength lines.

Due to the symmetry of the structure, the feeding network of the 8×8 planar array can be formed by putting this 1×4 array together. The simulated S parameters of the 5-port network for the 1×4 array are presented in Figure 9(b). It is clear from the figure that the input power is divided almost equally between the four antenna elements.

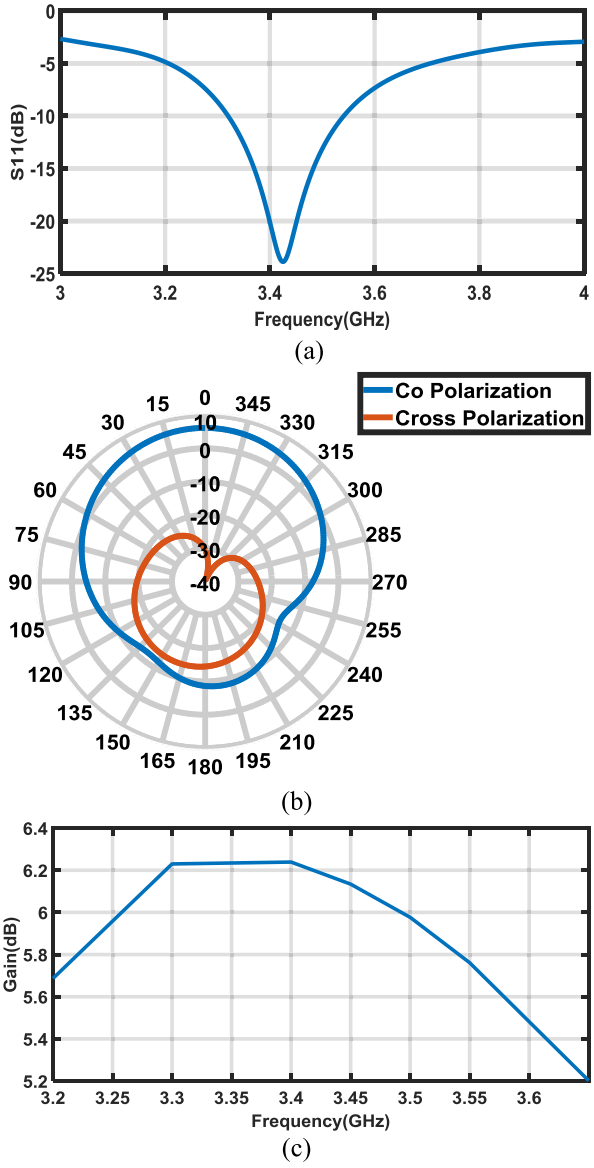

FIGURE 7. (a) Simulated S11 parameter, (b) radiation pattern in xoz plane at 3.4GHZ, and (c) max gain over frequency.

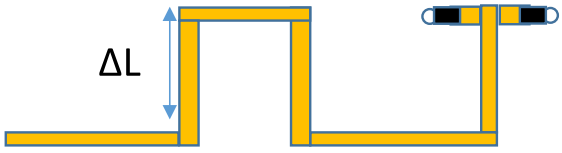

FIGURE 8. 1-bit phase shifter and phase delay line.

C. 1-BIT PLANAR ARRAY ANTENNA DESIGN

After designing the 1-bit antenna element, a 8×8 planar 1-bit array antenna with the proposed method is designed in this part. The top and bottom layers of the planar array antenna are shown in Figures 10(a), and (b), respectively. In the series feeding network, for the elements to be excited in phase, the length of the microstrip line between two adjacent elements must be λ_g. On the other hand, since in microstrip structures

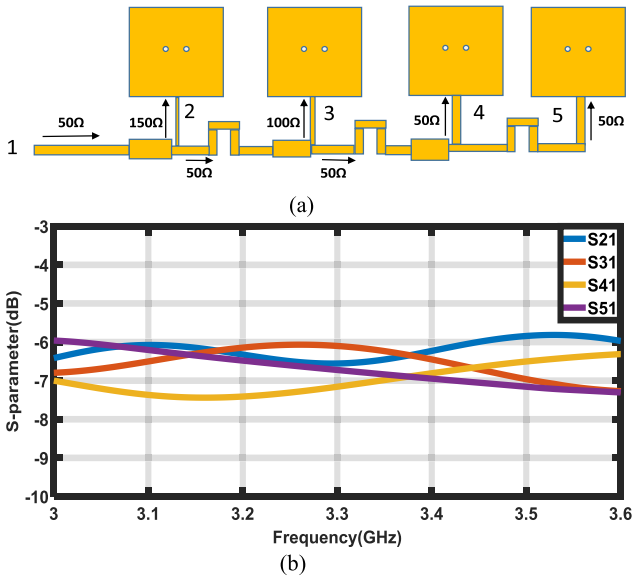

FIGURE 9. (a) Geometry of the 1-by-4 series-fed array with the phase delay line, and (b) Simulated S-parameters of the power divider.

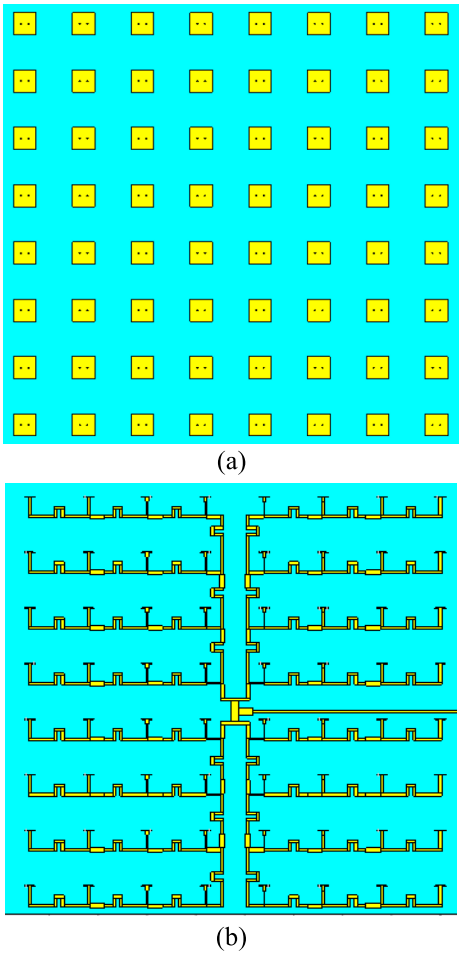

FIGURE 10. The geometry of 8*8 1-bit array antenna (a) top face array antenna, and (b) bottom face feeding network.

$\lambda_g < \lambda_0$, it is guaranteed that no grating lobe will be created up to a certain scanning angle. Therefore the inter-element spacing of 60 mm is adjusted.

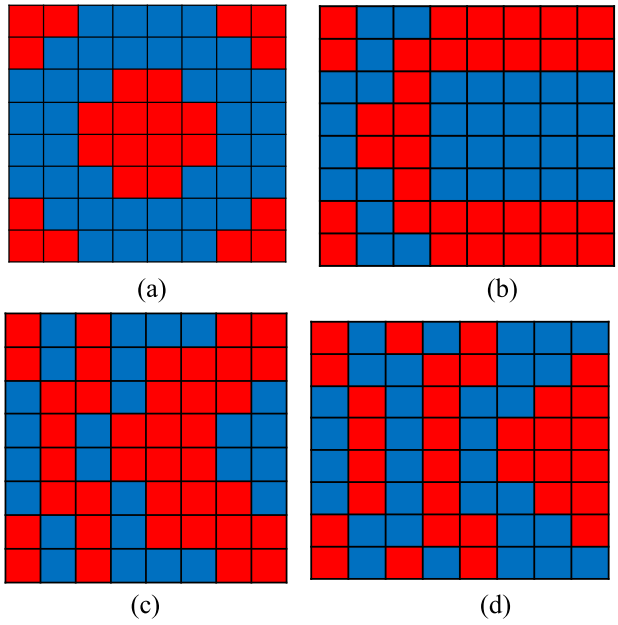

FIGURE 11. Quantized total phase distribution (a) (θ =0°, ϕ =0°), (b) (θ =15°, ϕ =0°), (c) (θ =30°, ϕ =0°), and (d) (θ =45°, ϕ =0°).

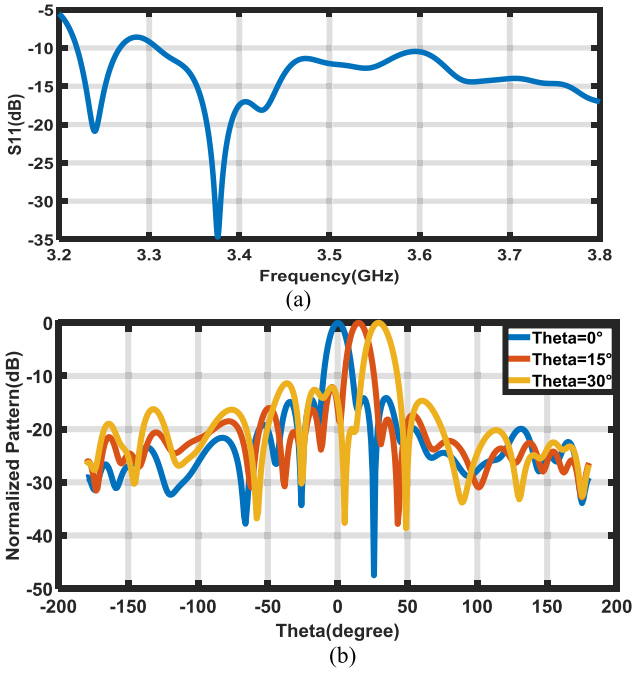

FIGURE 12. (a) Simulated S11 of 8*8 array antenna,(b) Simulated co-polarized radiation patterns of the planar array antenna for three beam scanning of θ = (0, 15, 30) °.

Figure 10(b) displays the series feeding network of the 8 × 8 planar array antenna with delay lines. To obtain the desired 8 × 8 array, the series feeding network is used to connect four 1 × 4 arrays to realize a 4 × 4 array. Finally, four 4 × 4 array are connected using a 1:4 power divider.

For steering the beam first we should calculate the phase of each element for the specified direction using equation (3) and then convert them to discrete values.

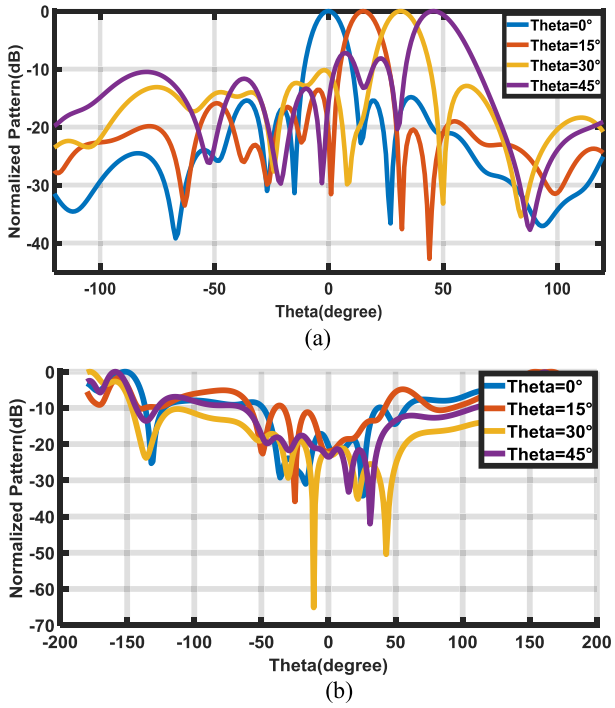

FIGURE 13. The simulation of the normalized (a) co-polarization and (b) cross-polarization radiation patterns of the planar array antenna for four beam scanning of θ = (0, 15, 30, 45) °.

Distribution of phase for $\theta = 0°, 15°, 30°, 45°$ are displayed in Figure 10. Figure 12(a) shows the return loss of the planar array antenna which is below -10 dB at the operating frequency of 3.4 GHz. Figure 12(b) shows the simulated realized gain patterns for the co-polarization component in the three beam scanning scenarios where the main beams are at $\theta = 0°, 15°, 30°$.

The realized gain values at 0°, 15°, and 30° are 19.6dB, 18.2dB, and 17.3dB, respectively, and the side lobe level in all these scanning angles is below -10 dB. Beyond 30°, the radiation patterns are unacceptable because of the high side lobes.

To achieve a greater scanning angle, the distance between the elements, and therefore the wavelength, should be reduced. This is possible by increasing the dielectric constant of the substrate. To verify this, the design is repeated for an FR4 substrate with $\varepsilon_r = 4.3$ and $\tan\delta = 0.02$. In this case, the inter-element spacing is selected as 48 mm. The simulation of the normalized co-polarization and cross-polarization radiation patterns of the planar array at different scanning angles is shown in Figure 13. As can be seen, in this case, the acceptable scanning angular range increases up to 45°. The realized gain values at 0°, 15°, 30°, and 45° are 11dB, 10.6dB, 9.8 dB, and 9.62 dB, respectively. The decrease in gain relative to F4B substrate is due to the high losses of the FR4 substrate.

IV. EXPERIMENTAL RESULTS

To verify the design a prototype of the proposed 8 × 8 reconfigurable 1-bit array antenna was fabricated and tested.

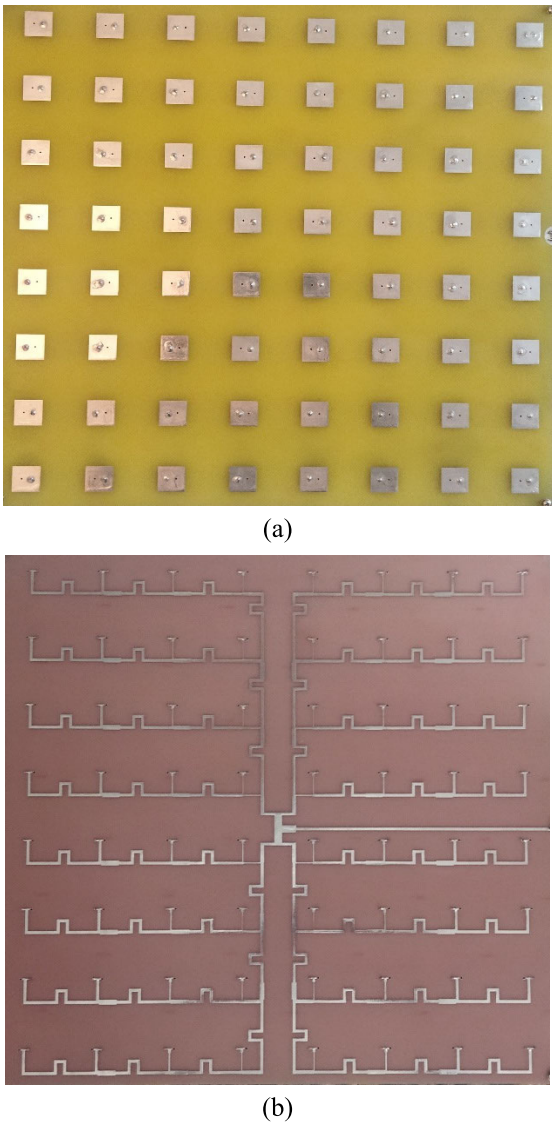

FIGURE 14. Photograph of the proposed 8 × 8 reconfigurable 1-bit array (a) front view (array antenna), and (b) back view (power divider).

TABLE 2. The comparison between simulated and measured radiation pattern parameters in scanning angles of 0° and 30°.

Scanning angle	Realized gain (dB)	Side lobe level (dB)	3-dB beamwidth (degree)	Main beam direction error (degree)
0	9.9/11	12.8/15.1	12.1/12.5	0.3/0
30	8.4/9.62	8.1/10.9	14.8/15.3	1/0

The substrate used was FR4 due to its low cost and availability. Two layers of FR4 substrate with thicknesses of 3.2 mm and 1mm, respectively, were utilized to fabricate the planar array. This structure includes 8 × 8 antenna elements, and the dimensions of the array are 380 × 380 mm^2. The top and bottom layers were connected with via holes with diameters of 1mm. The photograph of the fabricated planar array prototype is shown in Figure 14. The input port of the array is

TABLE 3. Comparisons between the proposed 1-bit planar array and the arrays in the references.

Reference	[6]	[10]	[20]	[15]	[16]	This work
Type	RA	TA	PA	PA	PA	PA
No of elements	14*14	20*20	48	1*8	4*8	8*8
Frequency(GHz)	11.5	29	11.725	3.65	12	3.45
Phase resolution	1bit	1bit	1bit	2bit	4bit	1bit
Max Gain(dB)	19.2	20.8	22	13.4	13.4	19.6
Scanning range	+/-60°	+/-60°	+/-30°	+/-49°	+/-45°	+/-45°
thickness	$7.3\lambda_0$	$6\lambda_0$	Not reported	$0.048\lambda_0$	$0.15\lambda_0$	$0.045\lambda_0$
feeding complexity	blockage, spillover loss, illumination loss	spillover loss, illumination loss	complex feed network due to sparse elements	complex feed network due to number of bits	complex feed network due to number of bits	simple

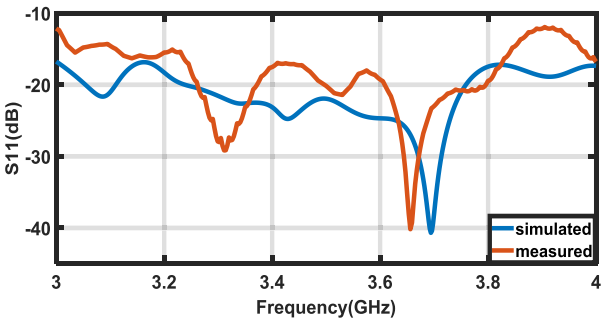

FIGURE 15. Simulated and measured results of S11.

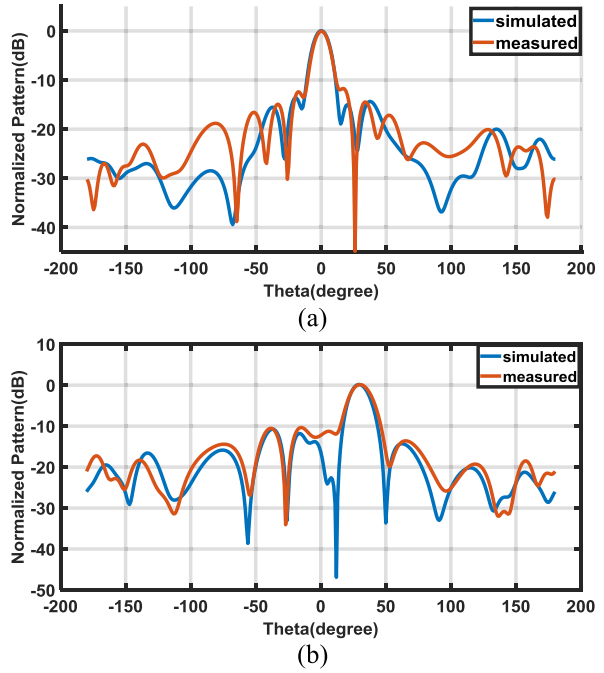

FIGURE 16. Simulated and measured normalized pattern for the scan angle of (a) (0, 0), and (b) (30°, 0) at 3.4GHz.

fed by an SMA connector. The ON/OFF states of PIN diodes that configure 0° and 180° phase shifts were implemented by the presence/absence of copper traces with widths of 0.3 mm on the bottom metallic layer. The measurement was done for two scanning angles of 0° and 30° at a frequency of 3.4 GHz. The simulation results were also added for comparison.

Figure 15 shows the simulated and measured results of return loss at 3-4 GHz. As can be seen, it is lower than −10 dB in the operating frequency of 3.4 GHz. The results of the radiation pattern for co-polarization at scanning angles of 0° and 30° are shown in Figure 16(a) and (b), respectively. The comparison between simulated and measured radiation pattern parameters is represented in Table 2. The difference between simulation and experimental results can be partly attributed to fabrication tolerances, uncertainties in measurements, and the dielectric properties of the FR4 material used for constructing the planar array antenna prototypes. Other reasons for the differences are the loss of the feeding SMA connector, the phase distribution of the power divider, and the phase quantization error.

A comparison of the performance of the proposed design with the existing arrays in the literature is provided in Table 3. As can be seen, the proposed structure does not have the disadvantages of the feed horn of transmitarray and reflectarray antennas, and it is much simpler than the feeding network of existing planar array structures. Additionally, when compared in terms of thickness, the proposed structure is very low profile.

V. CONCLUSION

In this paper, we presented a method for quantization lobe reduction in a 1-bit beam steering planar array antenna inspired by reflectarray feeding. In this technique, a predetermined phase is fed to each antenna element. The distribution of this predetermined phase is such that the further away from the center of the structure, the phase delay further increases. Each 1-bit element has a two-phase state (0/180°) that is controlled by two PIN diodes. For feeding the 8 × 8.1-bit array antenna, a series feeding line was used with U shape phase delay line for the realization of predetermined phases. Finally, the proposed array was fabricated and measured. The results show that the proposed array has a scan range between −45° and +45° with a maximum quantization lobe level of −9 dB and a gain variation of 1.5 dB. This work has a simpler feeding network than other 1-bit planar array antennas, which leads to the reduction of errors in the beam steering pattern. It also has a much smaller thickness than one-bit reflectarray antennas.

REFERENCES

[1] C.-M. Liu, S.-Q. Xiao, H.-L. Tu, and Z. Ding, "Wide-angle scanning low profile phased array antenna based on a novel magnetic dipole," *IEEE Trans. Antennas Propag.*, vol. 65, no. 3, pp. 1151–1162, Mar. 2017, doi: 10.1109/TAP.2016.2647711.

[2] G. Yang, J. Li, S. G. Zhou, and Y. Qi, "A wide-angle E-plane scanning linear array antenna with wide beam elements," *IEEE Antennas Wireless Propag. Lett.*, vol. 16, pp. 2923–2926, 2017, doi: 10.1109/LAWP.2017.2752713.

[3] G. Perez-Palomino, R. Florencio, J. A. Encinar, M. Barba, R. Dickie, R. Cahill, P. Baine, M. Bain, and R. R. Boix, "Accurate and efficient modeling to calculate the voltage dependence of liquid crystal-based reflectarray cells," *IEEE Trans. Antennas Propag.*, vol. 62, no. 5, pp. 2659–2668, May 2014, doi: 10.1109/TAP.2014.2308521.

[4] S. V. Hum, M. Okoniewski, and R. J. Davies, "Modeling and design of electronically tunable reflectarrays," *IEEE Trans. Antennas Propag.*, vol. 55, no. 8, pp. 2200–2210, Aug. 2007, doi: 10.1109/TAP.2007.902002.

[5] H. Kamoda, T. Iwasaki, J. Tsumochi, T. Kuki, and O. Hashimoto, "60-GHz electronically reconfigurable large reflectarray using single-bit phase shifters," *IEEE Trans. Antennas Propag.*, vol. 59, no. 7, pp. 2524–2531, Jul. 2011, doi: 10.1109/TAP.2011.2152338.

[6] H. Zhang, X. Chen, Z. Wang, Y. Ge, and J. Pu, "A 1-bit electronically reconfigurable reflectarray antenna in x band," *IEEE Access*, vol. 7, pp. 66567–66575, 2019, doi: 10.1109/ACCESS.2019.2918231.

[7] B. Xi, Y. Xiao, K. Zhu, Y. Liu, H. Sun, and Z. Chen, "1-bit wideband reconfigurable reflectarray design in Ku-band," *IEEE Access*, vol. 10, pp. 4340–4348, 2022, doi: 10.1109/ACCESS.2021.3117693.

[8] H. Luyen, J. H. Booske, and N. Behdad, "2-bit phase quantization using mixed polarization-rotation/non-polarization-rotation reflection modes for beam-steerable reflectarrays," *IEEE Trans. Antennas Propag.*, vol. 68, no. 12, pp. 7937–7946, Dec. 2020, doi: 10.1109/TAP.2020.3000517.

[9] M. Wang, S. Xu, F. Yang, N. Hu, W. Xie, and Z. Chen, "A novel 1-bit reconfigurable transmitarray antenna using a C-shaped probe-fed patch element with broadened bandwidth and enhanced efficiency," *IEEE Access*, vol. 8, pp. 120124–120133, 2020, doi: 10.1109/ACCESS.2020.3004435.

[10] L. D. Palma, A. Clemente, L. Dussopt, R. Sauleau, P. Potier, and P. Pouliguen, "Circularly-polarized reconfigurable transmitarray in Ka-band with beam scanning and polarization switching capabilities," *IEEE Trans. Antennas Propag.*, vol. 65, no. 2, pp. 529–540, Feb. 2017, doi: 10.1109/TAP.2016.2633067.

[11] C. Huang, W. Pan, X. Ma, and X. Luo, "1-bit reconfigurable circularly polarized transmitarray in X-band," *IEEE Antennas Wireless Propag. Lett.*, vol. 15, pp. 448–451, 2016, doi: 10.1109/LAWP.2015.2451697.

[12] F. Diaby, A. Clemente, R. Sauleau, K. T. Pham, and L. Dussopt, "2 bit reconfigurable unit-cell and electronically steerable transmitarray at *Ka*-band," *IEEE Trans. Antennas Propag.*, vol. 68, no. 6, pp. 5003–5008, Jun. 2020, doi: 10.1109/TAP.2019.2955655.

[13] H.-T. Chou, T.-W. Hsiao, and J.-H. Chou, "Active phased array of cavity-backed slot antennas with modified feeding structure for the applications of direction-of-arrival estimation," *IEEE Trans. Antennas Propag.*, vol. 66, no. 5, pp. 2667–2672, May 2018, doi: 10.1109/TAP.2018.2806419.

[14] L. Chang, Y. Li, Z. Zhang, and Z. Feng, "Reconfigurable 2-bit fixed-frequency beam steering array based on microstrip line," *IEEE Trans. Antennas Propag.*, vol. 66, no. 2, pp. 683–691, Feb. 2018, doi: 10.1109/TAP.2017.2776960.

[15] P. Liu, Y. Li, and Z. Zhang, "Circularly polarized 2 bit reconfigurable beam-steering antenna array," *IEEE Trans. Antennas Propag.*, vol. 68, no. 3, pp. 2416–2421, Mar. 2020, doi: 10.1109/TAP.2019.2939669.

[16] Z. X. Wang, H. Yang, R. Shao, J. W. Wu, G. Liu, F. Zhai, Q. Cheng, and T. J. Cui, "A planar 4-bit reconfigurable antenna array based on the design philosophy of information metasurfaces," *Engineering*, vol. 17, pp. 64–74, Oct. 2022, doi: 10.1016/j.eng.2022.03.019.

[17] H. Yang, F. Yang, S. Xu, M. Li, X. Cao, J. Gao, and Y. Zheng, "A study of phase quantization effects for reconfigurable reflectarray antennas," *IEEE Antennas Wireless Propag. Lett.*, vol. 16, pp. 302–305, 2017, doi: 10.1109/LAWP.2016.2574118.

[18] J. Hu, Z.-C. Hao, and Y. Wang, "A wideband array antenna with 1-bit digital-controllable radiation beams," *IEEE Access*, vol. 6, pp. 10858–10866, 2018, doi: 10.1109/ACCESS.2018.2801940.

[19] X. G. Zhang, W. X. Jiang, H. W. Tian, Z. X. Wang, Q. Wang, and T. J. Cui, "Pattern-reconfigurable planar array antenna characterized by digital coding method," *IEEE Trans. Antennas Propag.*, vol. 68, no. 2, pp. 1170–1175, Feb. 2020, doi: 10.1109/TAP.2019.2938678.

[20] M. C. Viganó, D. L. del Río, F. Bongard, and S. Vaccaro, "Sparse array antenna for Ku-band mobile terminals using 1 bit phase controls," *IEEE Trans. Antennas Propag.*, vol. 62, no. 4, pp. 1723–1730, Apr. 2014.

[21] A. K. Bhattacharyya, *Phased Array Antennas: Floquet Analysis, Synthesis, BFNs and Active Array Systems*. Hoboken, NJ, USA: Wiley, 2006.

[22] D. Pozar, "Finite phased arrays of rectangular microstrip patches," *IEEE Trans. Antennas Propag.*, vol. AP-34, no. 5, pp. 658–665, May 1986.

[23] H. Koo and S. Nam, "Mechanism and elimination of scan blindness in a T-printed dipole array," *IEEE Trans. Antennas Propag.*, vol. 68, no. 1, pp. 242–253, Jan. 2020.

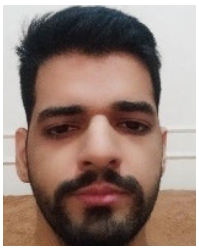

POORIA KABIRI received the B.S. degree in electrical engineering from Tafresh University, Iran, in 2019. He is currently pursuing the M.S. degree in electromagnetic fields and waves with the Department of Electrical Engineering, Iran University of Science and Technology (IUST), Tehran, Iran.

His current research interests include electromagnetics, antenna, microwaves, terahertz, and photonics.

MOHAMMAD KHALAJ-AMIRHOSSEINI was born in Tehran, Iran, in 1969. He received the B.Sc., M.Sc., and Ph.D. degrees in electrical engineering from the Iran University of Science and Technology (IUST), Tehran, in 1992, 1994, and 1998, respectively. He is currently a Professor with the School of Electrical Engineering, IUST. His current research interests include electromagnetics, microwaves, antennas, radio wave propagation, and electromagnetic compatibility.

ALI PESARAKLOO received the B.S. degree in electrical engineering from the Babol Noshirvani University of Technology (NIT), Iran, in 2011, and the M.Sc. degree in telecommunications engineering from the Iran University of Science and Technology (IUST), Tehran, Iran, in 2015, where he is currently pursuing the Ph.D. degree in electromagnetic fields and waves with the Department of Electrical Engineering.

His current research interests include electromagnetics, array antenna, metasurfaces, and active circuits.